Computational Materials Science 91 (2014) 192–199

Contents lists available at ScienceDirect

Computational Materials Science

journal homepage: www.elsevier.com/locate/commatsci

Cross-slip process in model Ni(Al) solid solution: An embedded-atom method study

Jun-Ping Du [a], Chong-Yu Wang [a,b,c,*], Tao Yu [a]

[a] Central Iron and Steel Research Institute, Beijing 100081, China
[b] Department of Physics, Tsinghua University, Beijing 100084, China
[c] The International Center for Materials Physics, Chinese Academy of Sciences, Shenyang 110016, China

ARTICLE INFO

Article history:
Received 3 October 2013
Received in revised form 2 April 2014
Accepted 29 April 2014
Available online 24 May 2014

Keywords:
Atomistic simulations
Embedded-atom potential
Cross-slip process
Model Ni(Al) solid solution

ABSTRACT

The cross-slip process of a screw dislocation in model Ni(Al) random solid solution is studied using the climbing image nudged elastic band method with an embedded-atom method potential. The average stacking fault energy of model Ni(Al) solid solution decreases with increasing Al concentration from 0 to 10 at.%. However, the average activation energy under zero stress shows an initial increase and then plateaus with increasing concentration of Al. The excess activation energy is determined by comparing with results from linear-elastic continuum theory. The short-range repulsive solute atom pair and its interaction with the dislocation provide the excess activation energy in the cross-slip process of model Ni(Al) solid solution.

1. Introduction

The cross-slip of screw dislocations is an essential process in the plastic deformation of metals [1]. The cross-slip process is closely related to hardening mechanisms, dislocation pattern formation, and dynamical recovery in metals [2]. During intermediate temperature creep deformation, the cross-slip process is the rate-controlling mechanism [3]. Zigzag-shaped dislocations in the γ phase of Ni-based superalloys are formed through cross-slip processes [4], and the evolution of the microtwins in the high temperature creep of the superalloys may also require cross-slip of the dislocations [5]. The cross-slip process has been investigated using the line-tension approximation, linear-elastic continuum theory, and atomistic modeling [2]. The advantage of atomistic modeling is that it does not require many assumptions to be made about the cross-slip process and gives physically based cross-slip models. Atomistic modeling of the cross-slip process has been performed for pure metals and intermetallic compounds, such as Cu [6], Ni [7] and $L1_2$–Ni_3Al [8]. The cross-slip mechanism in face-centered cubic (FCC) metals is most commonly described by the Escaig model [9]. Atomistic simulation of the cross-slip process in FCC metals has shown that the energy of the screw-like constriction is negative [6] and cross-slip can be inhibited by decreasing the stacking fault energy (SFE) of the FCC metal, such as the case of H in γ(Ni) [10–12]. Rao et al. [13–15] proposed a new cross-slip mechanism for a dislocation intersecting with forest dislocations in FCC metals using atomistic simulations. The cross-slip activation energy in Rao's model is lower than that in the Escaig model.

Recently, the glide of dislocations in Ni(Al) [16–18] and Al(Mg) [19] random solid solutions has been studied using molecular dynamics simulations. These studies found that a significant source of the hardening effect comes from the short-range interaction between solute and solute and the statistical nature of the distribution of the solutes in the random solid solution [16]. The working hardening of FCC alloys is correlated with the cross-slip activation energy of screw dislocations. The cross-slip activation energy has been given as a function of dislocation width based on linear-elastic continuum theory. However, the influence of the disordered distribution of solutes on the activation energy has not been studied. Therefore, it is important to investigate how the cross-slip process in the model solid solution is affected by the random distribution of solutes.

In this study, we consider the cross-slip in a model Ni(Al) solid solution with perfect disorder. The relationship between activation energy and dislocation width from atomistic simulation is compared with that from linear-elastic continuum theory to study the effect of random distribution of Al atoms on the activation energy. The diffusion of Al atoms and the short-range order in the alloy are beyond the scope of the present study.

* Corresponding author at: Department of Physics, Tsinghua University, Beijing 100084, China. Tel.: +86 10 6277 2782.
E-mail addresses: dujunping2001@gmail.com (J.-P. Du), cywang@mail.tsinghua.edu.cn (C.-Y. Wang), ytao012345@163.com (T. Yu).

http://dx.doi.org/10.1016/j.commatsci.2014.04.063
0927-0256/

2. Methodology

The minimum-energy pathway (MEP) of the cross-slip process was obtained using the climbing image nudged elastic band (CI-NEB) method [20,21] based on a string of replicas of the system connected one after another by springs. The spring constant was set at 1.0 eV/Å^2 [10]. Values of the spring constant ranging from 0.1 to 20 eV/Å^2 were tested in the simulations and it was found that the parameter does not affect the results. The convergence criterion for the CI-NEB method was selected to be the point when the force on the atoms was less than 0.01 eV/Å. The convergence criterion of 0.001 eV/Å was tested, and the difference in the energy barrier for the two force convergence criteria (0.01 and 0.001 eV/Å) was less than 0.01 eV. The dislocation configurations were visualized using the common neighbor analysis (CNA) method [22] and the software package OVITO [23]. The atomistic simulations were performed using the molecular dynamics Large-scale Atomic/Molecular Massively Parallel Simulator (LAMMPS) code [24].

The Ni–Al embedded atom method (EAM) potential [25] was used, which accurately gives the basic lattice properties of γ(Ni) and γ'(Ni$_3$Al). The potential also gives a reasonable value of the SFE of γ(Ni) and the planar fault energies of γ'(Ni$_3$Al). The relationship between the charge transfer, elastic constants, and host electron density of the EAM was considered when fitting the potential. By taking this relationship into account, the embedding energy in the potential has an important effect on the properties of the alloys, such as the planar fault energies of γ'(Ni$_3$Al). The Ni–Al EAM potential has also been used in the simulation of crack propagation in the Ni/Ni$_3$Al system [26]. The Vienna ab initio simulation package (VASP) [27] was used to verify the reliability of the potential. The projector augment wave method and the generalized gradient approximation parameterized by Perdew, Burke, and Ernzerhof [28] were used for the exchange correlation functional. All first-principles calculations were carried out in a spin-polarized mode. The cutoff energy of the plane-wave basis was 350 eV. The accuracy for electronic minimization was 10^{-4} eV, while the accuracy for ionic relaxation was 0.01 eV/Å.

3. Simulation results and discussion

3.1. Atomistic simulation of cross-slip process in model Ni(Al) random solid solution

3.1.1. Cross-slip process in model Ni(Al) random solid solution

A model of the cross-slip process was constructed in a cylindrical cell with a diameter of 14.4 nm and a length of 14.9 nm. The x and y axes were along the $[1\,2\,\bar{1}]$ and $[\bar{1}\,1\,1]$ directions, respectively, with free boundary conditions [10]. The z axis was along the [1 0 1] direction with periodic boundary conditions. The initial configuration of the screw dislocation was constructed by displacing the atoms according to the anisotropic elastic displacement field formula [29]. The dislocation line was set along the z axis. The system contained 258, 420 atoms. The distribution of Al atoms on the FCC lattice was completely random. The dissociation of the screw dislocations on the primary ($(\bar{1}\,1\,1)$) and cross-slip ($(1\,1\,\bar{1})$) planes are as follows:

$$\text{On the } (\bar{1}\,1\,1) \text{ plane}: \quad \frac{1}{2}[\bar{1}\,0\,\bar{1}] \rightarrow \frac{1}{6}[\bar{1}\,1\,\bar{2}] + \frac{1}{6}[\bar{2}\,\bar{1}\,\bar{1}], \tag{1}$$

$$\text{On the } (1\,1\,\bar{1}) \text{ plane}: \quad \frac{1}{2}[\bar{1}\,0\,\bar{1}] \rightarrow \frac{1}{6}[\bar{2}\,1\,\bar{1}] + \frac{1}{6}[\bar{1}\,\bar{1}\,\bar{2}]. \tag{2}$$

The dislocation configurations and MEP of the cross-slip process are shown in Fig. 1. The center positions of the extended dislocations in the initial and final states may not be on the central axis of the cylindrical cell because of the random distribution of Al atoms. The two partials in the initial state (see Fig. 1(a)) initially glide towards the central axis of the cylindrical cell (see Fig. 1(b)). Then, the two partials bow toward each other and form a constriction on the primary slip plane (see Fig. 1(c)). Next, two partials from the constriction are formed on the cross-slip plane, and the constriction dissociates into two half constrictions at the same time (see Fig. 1(d)). Because the direction of the dislocation line near the two half constrictions has changed, screw-like and edge-like partials are formed. The two corresponding half constrictions are referred to as the screw-like constriction and the edge-like constriction, respectively. The two half constrictions are then annihilated because of the periodic boundary condition. The screw dislocation is fully dissociated on the cross-slip plane (see Fig. 1(e)). Finally, the partials glide towards the final state (see Fig. 1(f)). From Fig. 1(g), the energy difference between Fig. 1(a) and (b) corresponds to the process of dislocation glide on the primary plane. Because the cross-slip activation energy is defined as the energy required for the formation and movement of a constriction, the dislocation configuration in Fig. 1(b), where a constriction is about to appear, is defined as a reference state for forward cross-slip (cross-slip from the initial state to the final state). Thus, the cross-slip activation energy is defined as $E_a = E_{\max} - E_r$, where $E_{\max}$ and E_r are the maximum energy in the energy path and the energy of the reference state, respectively. Similarly, another reference state and the corresponding activation energy for the reverse cross-slip process (cross-slip from the final state to the initial state) are also defined as shown in Fig. 1. The trends of MEP in the Ni(Al) solid solution are as follows: (1) the energy required to form a constriction (from Fig. 1(b) to (c)) is the lower bound of the activation energy required to complete the cross-slip process; (2) as the cross-slip progresses, the energy pathway randomly varies because of the random distribution of Al atoms. Because the activation energy is the maximum energy barrier in the energy pathway, the random increase in the energy pathway above the lower bound of the activation energy increases the value of the activation energy.

Because of the repulsive interaction between Al atoms, the close contact Al–Al atom pair is a high energy configuration. Al–Al atom pairs that cross the primary or cross-slip planes randomly break and form during the cross-slip process, so the energy path of the cross-slip process appears as a random walk. For the Ni(2 at.% Al) and Ni(10 at.% Al) solid solution, two constrained random solid solution models were constructed to test the effects of Al–Al atom pairs on the cross-slip process. The constrained random solid solutions were obtained by imposing zero Al concentration in one of the two $(\bar{1}\,1\,1)$ (or $(1\,1\,\bar{1})$) planes that cross the primary (or cross-slip) plane. Thus, Al–Al atom pairs crossing the primary and cross-slip planes are prevented in the cross-slip process. The energy pathways of the cross-slip process are shown in Fig. 2. From Fig. 2, the constrained random solid solutions have a smoother MEP and lower activation energy than the fully random solid solutions. The repulsive Al–Al atom pairs across the primary and cross-slip planes strongly affect the activation energy of the individual cross-slip process, especially for the condensed solid solution. In the condensed random solid solution, the Al atom clusters may also affect the cross-slip activation energy. However, the number of Al atom clusters is less than the number of Al–Al pairs. The size of the simulation model required to include enough atom clusters in the calculation of the average activation energy would be too large for the present atomistic simulation with the CI-NEB method. Atomistic simulations are more suited for studying the interaction between a dislocation and a few solute atom clusters within the dislocation core region where elasticity theory breaks down [30]. Therefore, we focus on the Al–Al pairs rather than larger clusters in this study.

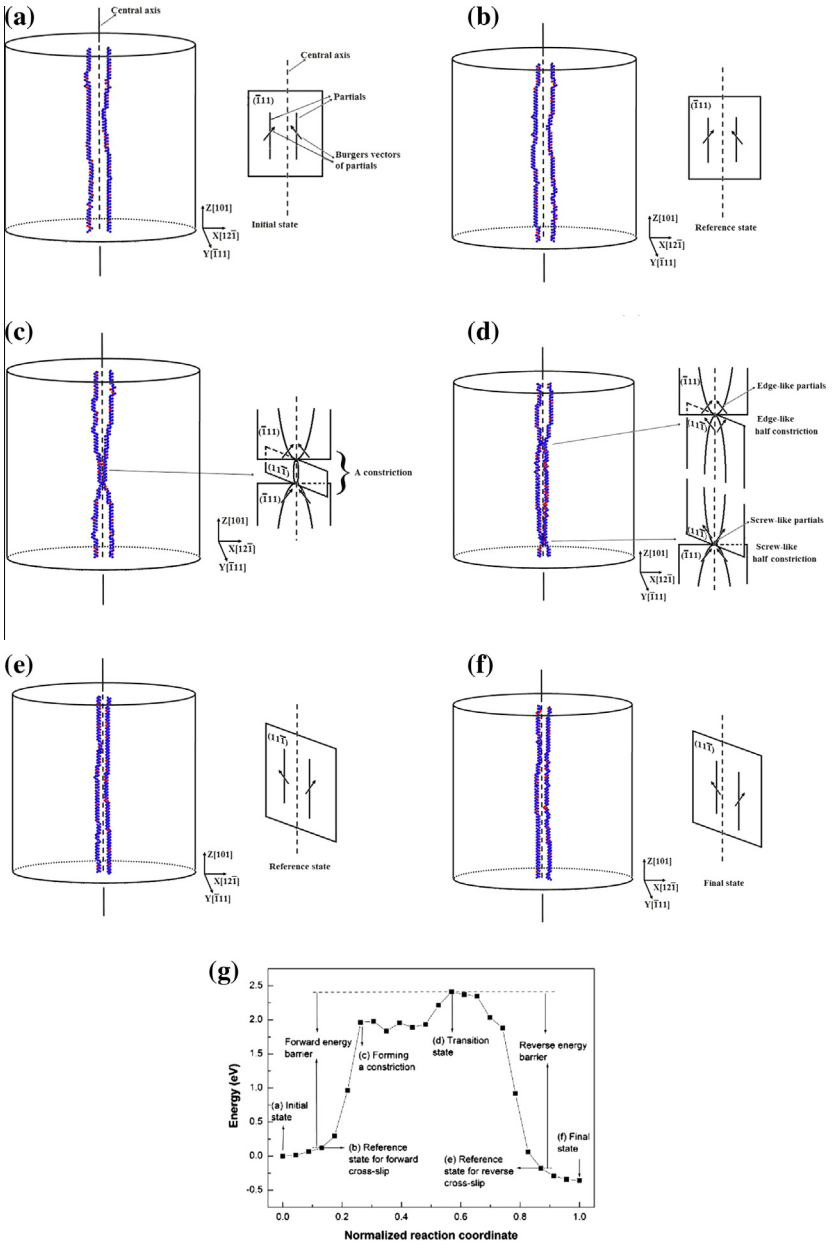

Fig. 1. Dislocation configurations for the cross-slip of a screw dislocation in model Ni(10 at.% Al) random solid solution. The red and blue circles denote Al and Ni atoms in the partials. (a) Initial state of the dislocation on the primary slip plane. (b) Reference state for the forward cross-slip. (c) Constriction formed in the dislocation. (d) Transition states of the cross slip process. Screw-like and edge-like half constrictions are shown. (e) Reference state for reverse cross-slip. (f) Configuration of the dislocation on the cross-slip plane. (g) MEP for the cross-slip process. The energies corresponding to states (a)–(f) are shown. (For interpretation of the references to color in this figure legend, the reader is referred to the web version of this article.)

3.1.2. Stacking fault energy and dislocation width

Decreasing the SFE of pure metals by alloying, which is accompanied with widening of the extended dislocations, is an important approach to inhibit cross-slip. The SFE of the model Ni(Al) random solid solution was calculated using a cubic cell with the size $10[\bar{1}\,\bar{1}\,2]a_0$, $30[1\,\bar{1}\,0]a_0$ and $10[1\,1\,1]a_0$ along the x, y and z directions, respectively, where a_0 is the equilibrium lattice parameter of the Ni(Al) random solid solution. Al atoms were randomly distributed in the FCC lattice. The free boundary condition was used in z direction and periodic boundary conditions were used in the x and y directions. The system energy E_1 was obtained by minimizing the energy of the system. Then, the system is divided into two equal parts along the z direction: the upper and the lower parts. The upper part was moved by a distance of $1/6[1\,1\,\bar{2}]a_0$, and a stacking fault is formed between the two parts. The system energy E_2 was obtained by minimizing the energy of the system with a stacking fault. The SFE of the Ni(Al) random solid solution was calculated by $E_{sf} = (E_2 - E_1)/S$, where S is the area of the stacking faults. The size of the system in the z direction is sufficiently large to prevent the influence of the surfaces on the SFE. For a given concentration of Al, 20 random solid solution models were created with different sets of random numbers and the corresponding SFEs were calculated. The SFEs as a function of the concentration of Al are shown in Fig. 3(a). Fig. 3(a) shows that the average stacking fault energy decreases with increasing Al concentration.

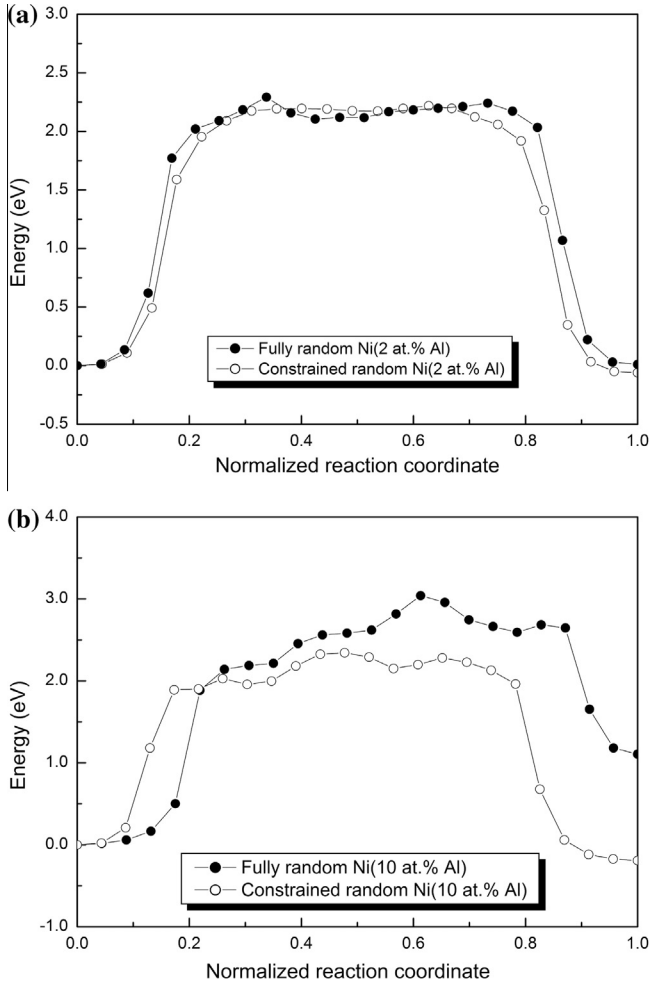

Fig. 2. Energy pathways of the cross-slip process for fully and constrained random (a) Ni(2 at.% Al) and (b) Ni(10 at.% Al) solid solutions.

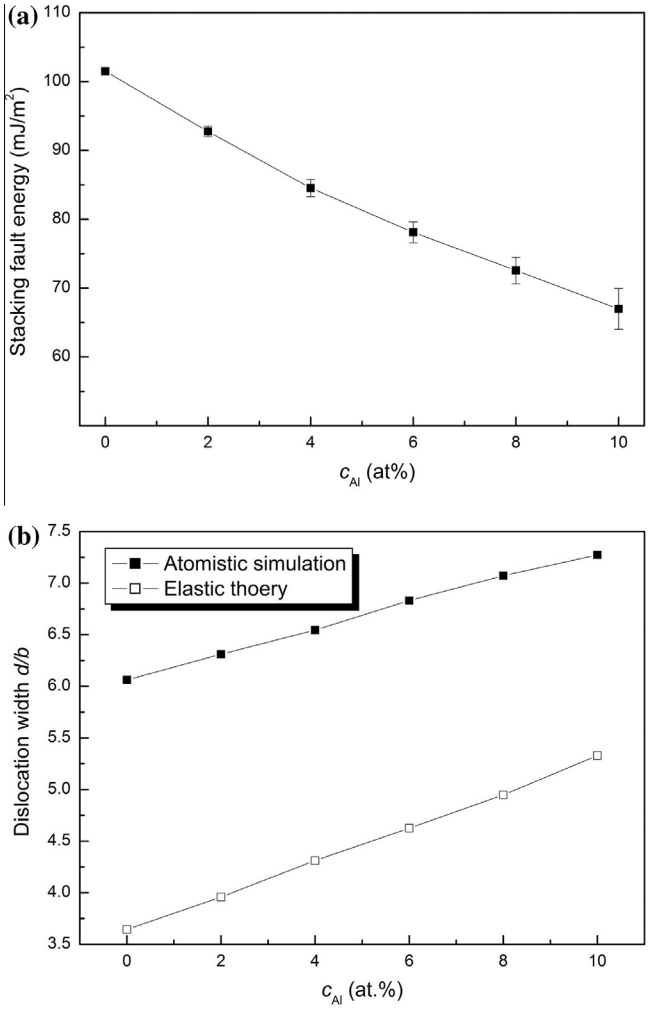

Fig. 3. (a) Stacking fault energies in model Ni(Al) random solid solution. The error bars correspond to the standard deviation. (b) Scaled width of dissociated screw dislocation (d/b) from both atomic simulations and elasticity theory, where d and b are the dislocation width and the length of Burgers vector, respectively.

From the atomistic simulations, the average dislocation width can be directly measured. The average distance between the partials in reference states is determined by $d = NS/(2l)$, where N is the number of atoms in stacking fault and dislocation cores, $S = \sqrt{3}a^2/4$ is the area per atom in the (1 1 1) plane, a is the lattice constant, and l is the length of the cylinder model in the z direction (see Fig. 1). The distance d between two partials of a screw dislocation can also be calculated with elasticity theory using the relationship [29]:

$$\frac{d}{b} = \frac{b}{8\pi E_{sf}}\left(K_s - \frac{1}{3}K_e\right), \tag{3}$$

where K_s and K_e are the functions of the elastic constants and E_{sf} is the stacking fault energy. The relationships between d/b and Al concentration calculated with the elasticity theory and from the atomistic simulation are shown in Fig. 3(b). From Fig. 3(b), the d/b monotonously increases with increasing Al concentration from 0 to 10 at.%. The values of d/b from the atomistic simulation are larger than those from the linear elasticity theory. This is because of two reasons: the free boundary conditions lead to image partial dislocations, which attract the partials to the surface in opposite directions, and the different relationship between the energy of system and the dislocation width during recombination of parallel partials into a perfect dislocation. Proville and Patinet [31] has calculated the dislocation width of edge dislocation in Ni(Al) random solid solution with periodic boundary conditions in the glide direction. Rao et al. [7] simulated the dislocation widths with flexible boundary conditions to prevent the influence of free surfaces based on two Ni potentials. The widths of dislocation from the atomistic simulations were also larger than those from elasticity theory.

3.1.3. Relationship between cross-slip activation energy and dislocation width

The average cross-slip activation energies as a function of $(d/b)\ln(2d/b)$ in pure Ni and model Ni(Al) solid solutions are shown in Fig. 4, where b and d are the length of Burgers vector and the distance between the partials of a screw dislocation, respectively. At least seven independent simulations were performed for each concentration of Al in Fig. 4. The average activation energies from the atomistic simulations are compared with those from the linear-elastic continuum theory (see Fig. 4). The cross-slip activation energy of FCC metals in linear-elastic continuum theory is given by [2]:

$$E_a \approx 2K_s b^3 \times 0.012\frac{d}{b}\ln\left(2\frac{d}{b}\right). \tag{4}$$

$K_s = \sqrt{c'_{44}c'_{55}}$, where c'_{44} and c'_{55} are the elastic constants of the FCC lattice under the coordinates $x = [0\,1\,0]$, $y = 1/\sqrt{2}[\bar{1}\,0\,1]$, and $z = 1/\sqrt{2}[1\,0\,1]$. The activation energy is linearly proportional to

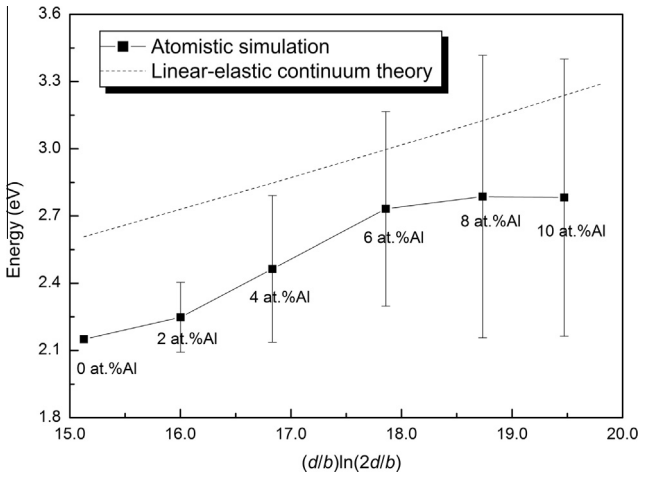

Fig. 4. Relationship between the activation energy and the scaled width of dissociated dislocation from atomistic simulations and linear-elastic continuum theory. The error bars indicate the standard deviation of the values.

the scaled dislocation width, $(d/b)\ln(2d/b)$, in linear-elastic continuum theory. The cross-slip activation energy in pure Ni is 2.15 eV. This value of the cross-slip activation energy is lower than the value given by Wen et al. [10] (3.07 eV) using the EAM potential for the H–Ni system [32,33]. This is because the SFE of γ(Ni) calculated with the present EAM potential (102 mJ/m^2) is higher than that calculated with the potential for the H–Ni system (89 mJ/m^2). The activation energies in the model Ni(Al) solid solution with a certain concentration of Al atoms are distributed in a wide energy range. From Fig. 4, the activation energy from the atomistic simulations deviates from the linear dependence of $(d/b)\ln(2d/b)$. In a dilute solid solution, such as from pure Ni to Ni(2 at.% Al) solid solution, the rate of change of activation energy as a function of $(d/b)\ln(2d/b)$ from the atomistic simulations is generally consistent with that from the linear-elastic continuum theory. However, owing to the random distribution of solutes, excess activation energies are shown in the solid solution with Al concentration from 2 to 6 at.%. For Al concentrations from 6 to 10 at.%, the activation energies are almost independent of the concentration and the width of dissociated dislocations. The trend of activation energy curve is influenced by the following three factors: (1) the probability for the screw dislocation to form low energy constriction (from Fig. 1(b) to (c)) increases with increasing Al concentration, which tends to decrease the activation energy; (2) after forming the constriction, the probability for the random walk of MEP to a higher energy barrier increases with increasing Al concentration; (3) the activation energy increases with increasing dislocation width (see Fig. 3(b)). The factor (1) is counteracted by the factors (2) and (3), which leads to the plateau on the relationship between activation energy and Al concentration.

The cross-slip process is related to the onset of stage III of strain hardening in FCC metals [34]. When the cross-slip of massive screw dislocations is activated, stage III begins and the strain hardening rate decreases. Both the random distribution of Al atoms and the lower SFE can increase the activation energy of cross-slip. Thus, the onset of dynamical recovery can be delayed by alloying.

3.2. Atomistic simulation of the effect of Al–Al atom pair on the cross-slip process

3.2.1. Energetic calculations of the Al–Al atom pair in FCC-Ni and at the SF

The relative stabilities of Al–Al atom pairs separated by second nearest-neighbor (2NN) or first nearest neighbor (1NN) distances in the FCC or SF regions were calculated using first-principles (VASP) and the EAM potential. A supercell model containing 96 Ni atoms (see Fig. 5) was used to study the relative stability of Al–Al atom pair configurations. Eight $(\bar{1}\,1\,1)$ planes were stacked along the z direction in the configuration CABCABAB. Periodic boundary conditions were applied along the x, y and z directions. The last four planes (ABAB) denote the SF region. The other four planes (CABC) denote the FCC region. Four configurations of Al–Al atom pairs were considered: Al–Al atom pairs in the FCC region separated by either 2NN (Fig. 5(a)) or 1NN (Fig. 5(b)) distances, and the Al–Al atom pairs in the SF region separated by either 2NN (Fig. 5(c)) or 1NN (Fig. 5(d)) distances. The models in Fig. 5(a)–(d) are referred to as FCC-2NN, FCC-1NN, SF-2NN, and SF-1NN, respectively. The binding energies of the four models ($E_b^{\mathrm{FCC-1NN}}$, $E_b^{\mathrm{FCC-2NN}}$, $E_b^{\mathrm{SF-1NN}}$, and $E_b^{\mathrm{SF-2NN}}$), were calculated by minimizing the total energy with respect to atomic positions, volume and shape of the supercells. The energies of relative stability for the Al–Al atom pair configurations for models FCC-1NN, FCC-2NN and SF-1NN with respect to that of SF-2NN were defined as:

$$\Delta E = E_b^{\mathrm{FCC/SF-1NN/2NN}} - E_b^{\mathrm{SF-2NN}}. \quad (5)$$

If $\Delta E > 0$, the Al–Al atom pair prefers to be separated by the 2NN distance in the SF region. The results calculated with VASP and the EAM potential are shown in Table 1. From Table 1, the

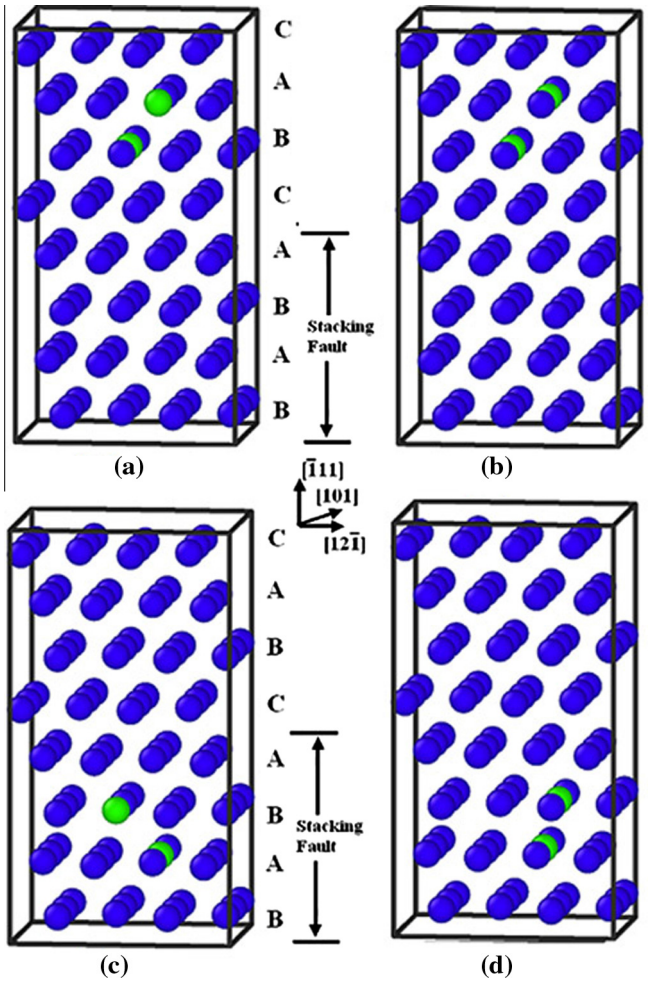

Fig. 5. Configuration of the supercell model containing Al–Al atom pairs. The blue and green spheres denote Ni and Al atoms, respectively. (a) Al–Al atom pair located in the FCC region separated by 2NN distance. (b) Al–Al atom pair located in the FCC region separated by 1NN distance. (c) Al–Al atom pair located in the SF region separated by 2NN distance. (d) Al–Al atom pair located in the SF region separated by 1NN distance.

Table 1
Energies (eV) of the relative stabilities of the Al–Al atom pairs in the models FCC-1NN, SF-1NN and FCC-2NN with respect to the model SF-2NN.

Method	FCC-1NN	SF-1NN	FCC-2NN
EAM	0.32	0.27	0.06
VASP	0.35	0.26	0.11

Al–Al atom pair prefers to be separated by a 2NN distance in the SF region compared with the other three configurations using both VASP and the EAM potential. The order of relative stability of the four models is: SF-2NN > FCC-2NN > SF-1NN > FCC-1NN, which means that the interatomic interaction between the two Al atoms is repulsive during the change in atomic configuration from SF-2NN to SF-1NN or FCC-1NN. The calculated results using the EAM potential are in agreement with those obtained from VASP, which demonstrates the reliability of results from the atomistic simulations using the EAM potential.

3.2.2. Effect of Al–Al atom pair on the cross-slip activation energy in γ(Ni)

The effect of an Al–Al atom pair on the cross-slip process was simulated with a 2NN Al–Al atom pair located in the SF region of the primary slip plane. Considering the symmetry, the Al–Al atom pair can be located at two pairs of sites, as shown in Fig. 6. The corresponding models are referred to as Model(1) and Model(2). In Model(1) the Al–Al atom pair is located in the SF region both before and after the cross-slip process. In Model(2), the 2NN Al–Al atom pair is initially located in the SF region of the primary glide plane and becomes a 1NN Al–Al atom pair in the FCC region after the cross-slip process. The initial cross-slip pathway is set so that one of the half constrictions comes into contact with the Al–Al atom pair first. The MEPs for the cross-slip processes in Model(1), Model(2), and γ(Ni) are shown in Fig. 7. The calculated activation energies for Model(1), Model(2), and γ(Ni) are listed in Table 2. Table 2 shows that the cross-slip activation energies are almost equal for the edge-like and screw-like constriction when first coming into contact with the Al–Al atom pair. The cross-slip activation energies for Model(1) and Model(2) are approximately 2.37 and 2.34 eV, respectively. The cross-slip activation energy including the Al–Al atom pair is approximately 0.2 eV higher than the activation energy of γ(Ni). The dislocation configuration at the saddle point of the MEP was relaxed to ensure that the activation energy increment is correct. For comparison, the influence of an isolated Al atom on the cross-slip process was simulated. One Al atom of the Al–Al atom pair in Model(2) was replaced by a Ni atom, and the edge-like constriction was selected to come into contact with the remaining Al atom first. The cross-slip activation energy of the model containing an isolated Al atom was found to be almost equal to that of the γ(Ni) system (as shown in Fig. 7 and Table 2). This shows that the influence of Al–Al atom pairs on the cross-slip

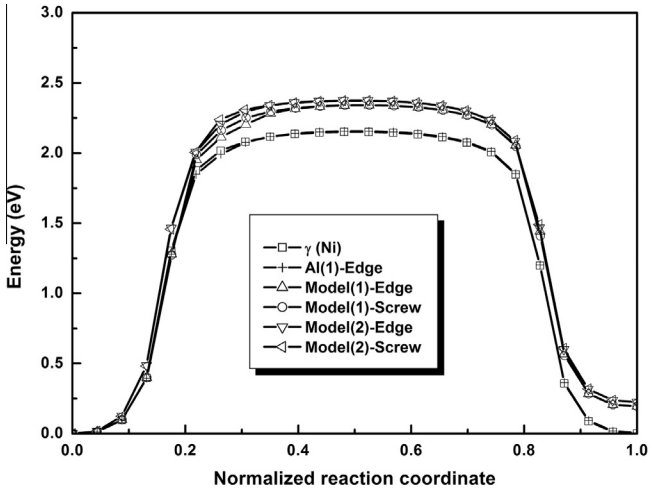

Fig. 7. Minimum energy pathway of cross-slip process for pure Ni (γ(Ni)), an isolated Al atom in the SF region (Al(1)) and 2NN Al–Al atom pair in the SF region (Model(1) and Model(2)). "Edge" and "Screw" denote that the edge-like or screw-like constriction comes into contact with the Al–Al atom pair first, respectively.

Table 2
Cross-slip activation energies of γ(Ni), γ(Ni) containing an isolated Al atom in the SF region (Al(1)), and γ(Ni) containing an Al–Al atom pair in the SF region (Model(1) and Model(2)) The suffixes "Edge" and "Screw" denote that the edge-like or screw-like constriction comes into contact with the Al–Al atom pairs first, respectively. The activation energy difference with respect to the activation energy of γ(Ni) is given in the parentheses.

Models	Activation energy (eV)
γ(Ni)	2.15
Al(1)-Edge	2.16 (0.01)
Model(1)-Edge	2.37 (0.22)
Model(1)-Screw	2.37 (0.22)
Model(2)-Edge	2.34 (0.19)
Model(2)-Screw	2.34 (0.19)

activation energy is much greater than that of the interaction between an isolated Al atom and the dislocation.

One Al–Al atom pair in γ(Ni) has little influence on the SFE of the system. Thus, we can analyze the chemical effect of the Al–Al atom pair on the cross-slip activation energy without changing the SFE. To accomplish this, we calculated the energy contributions from the atoms located between the $(00nb)$ and the $(00(n+1)b)$ planes (where b is the magnitude of the Burgers vector and n = 0–23.) to the total energy of the intermediate states, as shown in Fig. 8. These energy contributions are calculated using $\delta E_i(nb) = E_i(nb) - E_0(nb)$, where $E(nb)$ are the total energies of atoms that are located between the $(00nb)$ and $(00(n+1)b)$ planes, and the subscripts i and 0 denote the ith replica and the

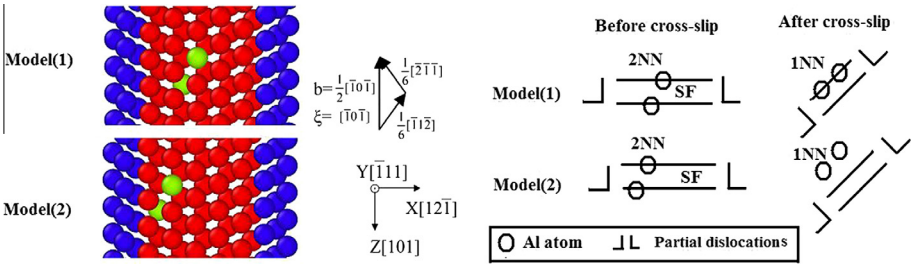

Fig. 6. Configurations of Al–Al atom pairs in the screw dislocation. The atoms in the dislocation core and stacking fault are colored blue and red, respectively. The green atoms are substituted by Al atoms. (For interpretation of the references to color in this figure legend, the reader is referred to the web version of this article.)

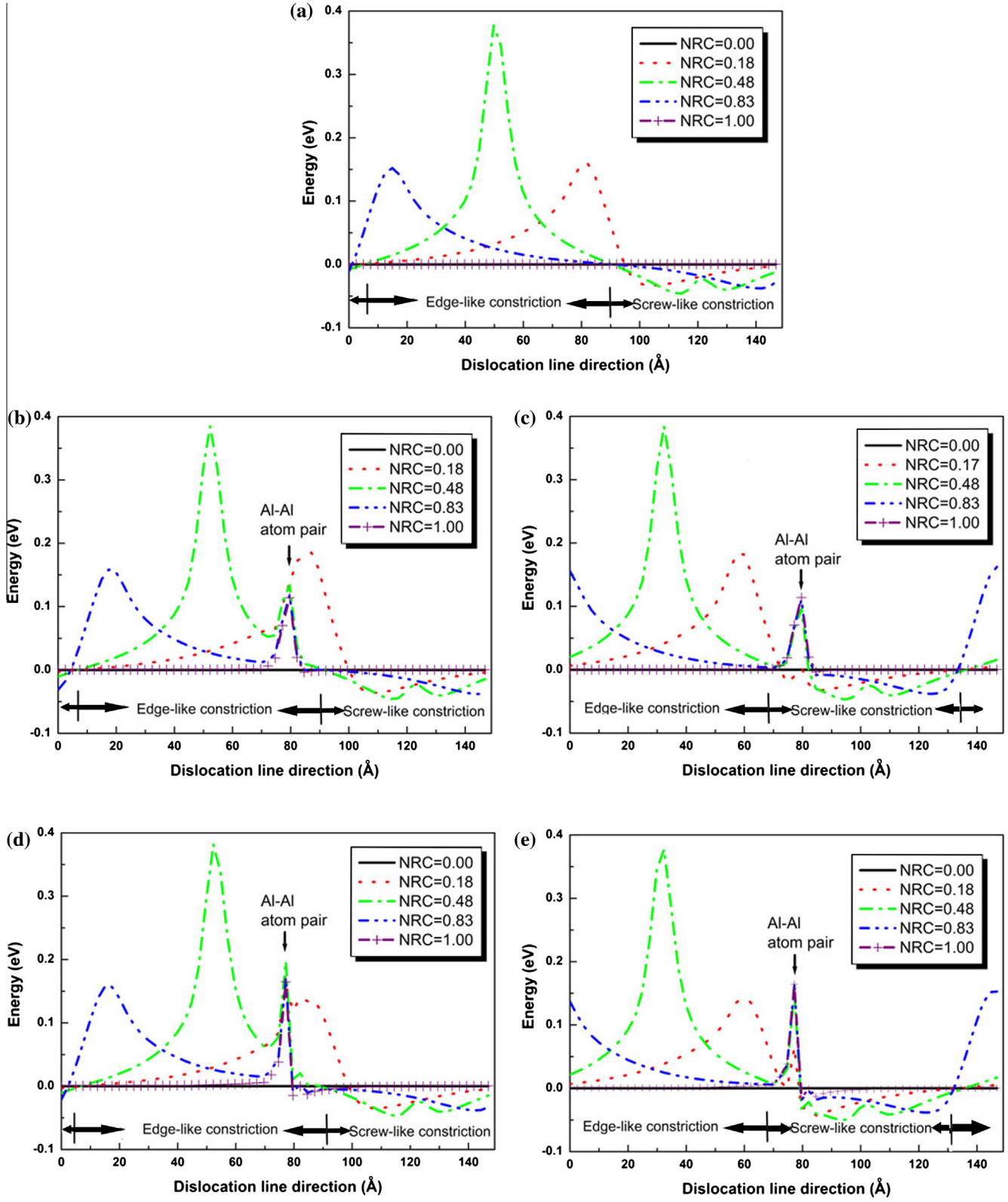

Fig. 8. Contributions of the intermediate states to the total energy (labeled by normalized reaction coordinates (NRC)) from atoms located at two (1 1 0) planes separated by Burgers vector ***b*** for the models (a) γ(Ni), (b) Model(1)-Edge, (c) Model(1)-Screw, (d) Model(2)-Edge, and (e) Model(2)-Screw. The plot of NRC = 0.0 defines the zero point of the energy.

initial state, respectively. From Fig. 8(a), the edge-like constriction has a positive energy and the screw-like constriction has a negative energy in γ(Ni). The sum of the positive and the negative energies at the saddle point in the MEP is the cross-slip activation energy. From Fig. 8(b)–(e), either the edge-like constriction energy or the screw-like constriction energy increases relative to the energy of γ(Ni) as the constriction passes through the Al–Al atom. The chemical effect of Al–Al atom pair on the cross-slip activation energy is

different from that of the decreasing SFE by the solute element. Both the edge-like and screw-like constriction energies change with decreasing SFE [12]. In contrast, the chemical effect of the Al–Al atom pair increases either the edge-like or the screw-like constriction energies (see Fig. 8).

4. Conclusions

The CI-NEB method and EAM potential were used to study the cross-slip process in a model Ni(Al) random solid solution. The MEP in the cross-slip process shows random walk behavior because of the random distribution of Al atoms. The average activation energy of the cross-slip process rapidly increases with increasing concentration of Al atoms, and reaches a maximum value at a concentration of 6 at.% Al. The dependence of the activation energy on the scaled width of dislocation, $(d/b)\ln(2d/b)$, deviates from the linear relationship predicted by linear-elastic continuum theory. The short-range repulsive Al–Al atom pairs and their interaction with the dislocations provide the excess activation energy. The chemical effect of repulsive Al–Al atom pairs on the cross-slip is localized around the atom pair, while the effect of the lower SFE on the cross-slip extends throughout the entire SF. The cross-slip process in the plastic deformation of random Ni(Al) solid solution should be inhibited by the randomly distributed solutes.

Acknowledgments

The authors thank Professor Wei-Hua Wang for helpful discussions. This work was supported by the National Basic Research Program of China (Grant No. 2011CB606402) and the National Natural Science Foundation of China (Grant No. 51071091). Simulations were carried out on the "Explorer 100" cluster system of Tsinghua National Laboratory for Information Science and Technology, China.

References

[1] A.S. Argon, Strengthening Mechanisms in Crystal Plasticity, Oxford University Press, 2008.
[2] W. Püschl, Prog. Mater. Sci. 47 (2002) 415–461.
[3] J. Friedel, Rev. Phys. Appl. 12 (1977) 1649–1654.
[4] T. Link, A. Epishin, B. Fedelich, Philos. Mag. 89 (2009) 1141–1159.
[5] R.R. Unocic, N. Zhou, L. Kovarik, C. Shen, Y. Wang, M.J. Mills, Acta Mater. 59 (2011) 7325–7339.
[6] T. Rasmussen, K.W. Jacobsen, T. Leffers, O.B. Pedersen, S.G. Srinivasan, H. Jónsson, Phys. Rev. Lett. 79 (1997) 3676–3679.
[7] S. Rao, T.A. Parthasarthy, C. Woodward, Philos. Mag. A 79 (1999) 1167–1192.
[8] T.A. Parthasarathy, D.M. Dimiduk, Acta Mater. 44 (1996) 2237–2247.
[9] B. Escaig, Phys. Stat. Sol. (b) 28 (1968) 463–741.
[10] M. Wen, S. Fukuyama, K. Yokogawa, Phys. Rev. B 69 (2004) 174108.
[11] M. Wen, S. Fukuyama, K. Yokogawa, Scripta Mater. 52 (2005) 959–962.
[12] M. Wen, S. Fukuyama, K. Yokogawa, Phys. Rev. B 75 (2007) 144110.
[13] S.I. Rao, D.M. Dimiduk, J.A. El-Awady, T.A. Parthasarathy, M.D. Uchic, C. Woodward, Philos. Mag. 89 (2009) 3351–3369.
[14] S.I. Rao, D.M. Dimiduk, J.A. El-Awady, T.A. Parthasarathy, M.D. Uchic, C. Woodward, Acta Mater. 58 (2010) 5547–5557.
[15] S.I. Rao, D.M. Dimiduk, T.A. Parthasarathy, J. El-Awady, C. Woodward, M.D. Uchic, Acta Mater. 59 (2011) 7135–7144.
[16] E. Rodary, D. Rodney, L. Proville, Y. Bréchet, G. Martin, Phys. Rev. B 70 (2004) 054111.
[17] L. Proville, D. Rodney, Y. Brechet, G. Martin, Philos. Mag. 86 (2006) 3893–3920.
[18] S. Patinet, L. Proville, Phys. Rev. B 78 (2008) 104109.
[19] S. Patinet, L. Proville, Philos. Mag. 91 (2011) 1581–1606.
[20] G. Henkelman, B.P. Uberuaga, H. Jónsson, J. Chem. Phys. 113 (2000) 9901–9904.
[21] G. Henkelman, H. Jónsson, J. Chem. Phys. 113 (2000) 9978–9985.
[22] D. Faken, H. Jónsson, Comput. Mater. Sci. 2 (1994) 279–286.
[23] A. Stukowski, Modell. Simul. Mater. Sci. Eng. 18 (2010) 015012.
[24] S. Plimpton, J. Comp. Phys. 117 (1995) 1–19. http://lammps.sandia.gov.
[25] J.P. Du, C.Y. Wang, T. Yu, Modell. Simul. Mater. Sci. Eng. 21 (2013) 015007.
[26] Z.G. Liu, C.Y. Wang, T. Yu, Modell. Simul. Mater. Sci. Eng. 21 (2013) 045009.
[27] G. Kresse, J. Hafner, Phys. Rev. B 47 (1993) 558–561.
[28] J.P. Perdew, K. Burke, M. Ernzerhof, Phys. Rev. Lett. 77 (1996) 3865–3868.
[29] J.P. Hirth, J. Lothe, Theory of Dislocations, John Wiley & Sons, 1982.
[30] D.J. Bacon, Y.N. Osetsky, D. Rodney, Dislocation-obstacle interactions at the atomic level, in: J.P. Hirth, L. Kubin (Eds.), Dislocations in Solids, North-Holland, Oxford, 2009, pp. 1–90.
[31] L. Proville, S. Patinet, Phys. Rev. B 82 (2010) 054115.
[32] J.E. Angelo, N.R. Moody, M.I. Baskes, Modell. Simul. Mater. Sci. Eng. 3 (1995) 289–307.
[33] M.I. Baskes, X. Sha, J.E. Angelo, N.R. Moody, Modell. Simul. Mater. Sci. Eng. 5 (1997) 651–652.
[34] F.R.N. Nabarro, Acta Metall. 37 (1989) 1521–1546.